

Fast Geometric Transformations on Quantum Images

Phuc Q. Le^{*}, Abdullahi M. Iliyasu[†], Fangyan Dong[‡], Kaoru Hirota[§]

Abstract—Circuits to achieve geometric transformations including two-point swapping, flip, co-ordinate swapping, orthogonal rotations and their variants on N -sized quantum images are proposed based on the basic quantum gates; NOT, CNOT and Toffoli gates. The complexity of the circuits is $O(\log^2 N)$ for two-point swapping and $O(\log N)$ for flip, co-ordinate swapping and orthogonal rotations. The results indicate that local operations like two-point swapping are slower than global operations like flip, co-ordinate swapping, and orthogonal rotations in quantum image processing. This is in contrast to performing such operations in classical image processing where the local operations are faster. All the proposed transformations are confirmed by simulation on a classical computer. With their low complexity, these geometric transformations can be used as the major components to build circuits for other applications on quantum images.

Keywords: quantum computation, image processing, geometric transformation, complexity, quantum circuit

1 Introduction

In recent years quantum computation and quantum information have generated so much interest especially with the prospect of employing its insights to empower our knowledge on information processing. In 1994 Peter Shor[16] discovered a quantum algorithm to factor integer numbers in polynomial time. This was closely followed by Grover's quadratic speed-up database search algorithm[7]

on the quantum computation model. These results and the unavoidably inefficient simulation of quantum physics on classical computers[5] provide the solid evidence of the strength of quantum computers over classical ones.

In quantum circuit models of computation, designing such circuits is necessary to realize and analyze any quantum algorithm. It is well known that any unitary operation or quantum algorithm can be decomposed into a circuit consisting a succession of basic unitary gates that act on one or two qubits only. Many elementary gates including single qubit gates, controlled-NOT or CNOT and Toffoli gates for quantum computation was introduced in [1]. Physical implementations of the qubit and these gates are available from many approaches [14], [15,Chapter 7].

One of the most active fields in quantum computation and information is quantum image processing. Quantum signal processing transformations such as Fourier[15], wavelet[6], and discrete cosine[8],[17] are proven to be more efficient than their classical versions. Using these efficient operations for image processing applications previously inefficient approaches involving classical operations are realizable.[2]. Parallelism in quantum computation can speed up many image processing tasks which have characteristics of parallelism[12]. Some concepts of quantum images have been proposed like Qubit Lattice[18],[19], Real Ket[9] and Flexible Representation of Quantum Images(FRQI)[12] in order to make the connection between quantum algorithms and image processing applications. Some impossible processing operations on quantum computers[10] indicate the fundamental difference between quantum and classical operations. To design fast algorithms for quantum image processing, we need to extend our knowledge on fundamental and efficient operations since only few of them are known as mentioned earlier.

Fast geometric transformations such as the two-point swapping, flip, co-ordinate swapping, orthogonal rotations and their variants for quantum images, specifically those based on the FRQI representation, are proposed using the basic quantum gates, NOT, CNOT and Toffoli gates. For an N -sized image, the detailed analysis of quantum circuits show that the complexity is $O(\log^2 N)$ for two-point swapping and $O(\log N)$ for the other operations. The two-point swapping operation is powerful

^{*}Corresponding author. Department of Computational Intelligence and Systems Science, Interdisciplinary Graduate School of Science and Engineering, Tokyo Institute of Technology, G3-49, 4259 Nagatsuta, Midoriku, Yokohama 226-8502, Japan. Tel.: +81-45-924-5686/5682, Fax: +81-45-924-5676, E-mail: phucclq@hrt.dis.titech.ac.jp

[†]Department of Computational Intelligence and Systems Science, Interdisciplinary Graduate School of Science and Engineering, Tokyo Institute of Technology, G3-49, 4259 Nagatsuta, Midoriku, Yokohama 226-8502, Japan. E-mail: iliyasu@hrt.dis.titech.ac.jp

[‡]Department of Computational Intelligence and Systems Science, Interdisciplinary Graduate School of Science and Engineering, Tokyo Institute of Technology, G3-49, 4259 Nagatsuta, Midoriku, Yokohama 226-8502, Japan. E-mail: tou@hrt.dis.titech.ac.jp

[§]Department of Computational Intelligence and Systems Science, Interdisciplinary Graduate School of Science and Engineering, Tokyo Institute of Technology, G3-49, 4259 Nagatsuta, Midoriku, Yokohama 226-8502, Japan. E-mail: hirota@hrt.dis.titech.ac.jp

since it can be built by arbitrary geometric transformations, but it is slower than the others. This fact is in contrast to their performance in classical versions but it agrees with the parallelism characteristic of quantum computation. In terms of their effect on images, the local transformations are slower than global ones among quantum image processing operations. The orthogonal rotations are the first examples of applying a succession of quantum transformations to create new applications on quantum image processing. The experiments by simulation of the quantum operations on classical computers confirm the feasibility of all of the proposed transformations. The fast geometric transformations can be used as efficient blocks to design other quantum image processing algorithms.

The rest of the paper is organized as follows. We start with a brief overview of the the flexible representation of quantum images (FRQI) and the general framework for geometric transformations on FRQI. In subsequent sections the various definitions, lemmas, theorems and proofs for the two-point swap gate, flip gate, co-ordinate swapping, orthogonal rotation gates, and their variants are presented. Experimental results to prove the realization of the geometric transformations and their feasibility are discussed in section 6. Discussion of future work and concluding remarks are found in section 7.

2 Representation of quantum images and general framework of geometric transformations

We start by introducing the notations used in this paper which has been used in a wide range of quantum computation literature[15]. The state of a quantum system is described as a vector in a Hilbert space which is called a ket in Dirac or quantum mechanical notation. The ket and its adjoint, bra, notations are defined as follows;

$$|u\rangle = \begin{bmatrix} u_0 \\ u_1 \\ \vdots \\ u_{n-1} \end{bmatrix}, u_i \in \mathbb{C}, i = 0, 1, \dots, n - 1,$$

$$\langle u| = |u\rangle^\dagger = [u_0^\dagger u_1^\dagger \dots u_{n-1}^\dagger].$$

The notation for the tensor or Kronecker product, \otimes , is used to express the composition of quantum systems. The tensor product of two matrices A and B is defined as follows;

$$A = \begin{bmatrix} a_{11} & a_{12} & \dots & a_{1m} \\ a_{21} & a_{22} & \dots & a_{2m} \\ \vdots & \vdots & \ddots & \vdots \\ a_{n1} & a_{n2} & \dots & a_{nm} \end{bmatrix},$$

$$B = \begin{bmatrix} b_{11} & b_{12} & \dots & b_{1q} \\ b_{21} & b_{22} & \dots & b_{2q} \\ \vdots & \vdots & \ddots & \vdots \\ b_{p1} & b_{p2} & \dots & b_{pq} \end{bmatrix},$$

$$A \otimes B = \begin{bmatrix} a_{11}B & a_{12}B & \dots & a_{1m}B \\ a_{21}B & a_{22}B & \dots & a_{2m}B \\ \vdots & \vdots & \ddots & \vdots \\ a_{n1}B & a_{n2}B & \dots & a_{nm}B \end{bmatrix},$$

where

$$a_{ij}B = \begin{bmatrix} a_{ij}b_{11} & a_{ij}b_{12} & \dots & a_{ij}b_{1q} \\ a_{ij}b_{21} & a_{ij}b_{22} & \dots & a_{ij}b_{2q} \\ \vdots & \vdots & \ddots & \vdots \\ a_{ij}b_{p1} & a_{ij}b_{p2} & \dots & a_{ij}b_{pq} \end{bmatrix}, \forall i, j.$$

The short notation for tensor product $|u\rangle \otimes |v\rangle$ of two vectors or two kets, $|u\rangle$ and $|v\rangle$, is $|uv\rangle$ or $|u\rangle|v\rangle$ and we use $A^{\otimes n} = A \otimes A \otimes \dots \otimes A$ to denote the tensor product of matrix A for n times.

The representation of quantum images, which enables the application of unitary transformations, was proposed in [12]. This proposal integrates information about colors and their corresponding positions in an image into a quantum state having its formular as in (1)

$$|I(\theta)\rangle = \frac{1}{2^n} \sum_{k=0}^{2^{2n}-1} |c_k\rangle \otimes |k\rangle, \tag{1}$$

$$|c_k\rangle = \cos \theta_k |0\rangle + \sin \theta_k |1\rangle, \tag{2}$$

$$\theta_k \in \left[0, \frac{\pi}{2}\right], k = 0, 1, \dots, 2^{2n} - 1, \tag{3}$$

where \otimes is the tensor product notation, $|0\rangle, |1\rangle$ are 2-D computational basis quantum states, $|k\rangle, k = 0, 1, \dots, 2^{2n} - 1$ are 2^{2n} -D computational basis quantum state and $\theta = (\theta_0, \theta_1, \dots, \theta_{2^{2n}-1})$ is the vector of angles encoding colors. There are two parts in the FRQI representation of an image; $|c_k\rangle$ and $|k\rangle$ which encode information about the colors and their corresponding positions in the image, respectively.

For the 2-D images, the position information $|k\rangle$ includes two parts, the vertical and horizontal co-ordinates. In $2n$ -qubit systems for preparing quantum images, or $2n$ -qubit images, the vector $|k\rangle$

$$|k\rangle = |y\rangle|x\rangle = |y_{n-1}y_{n-2} \dots y_0\rangle|x_{n-1}x_{n-2} \dots x_0\rangle,$$

$$x_i, y_i \in \{0, 1\},$$

for every $i = 0, 1, \dots, n$, which encodes the first n -qubit $y_{n-1}, y_{n-2}, \dots, y_0$ the vertical location and the second n -qubit $x_{n-1}, x_{n-2}, \dots, x_0$ encodes the horizontal location information as shown in Fig. 1.

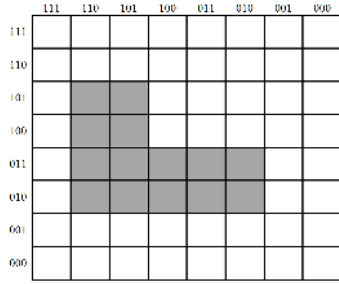


Figure 1: Vertical and horizontal coordinates encoded in qubits

Geometric transformations are the operations which are performed based on the geometric information of images, i.e., information about the position of every point in the image. Therefore, these transformations, G_I , on FRQI quantum images can be defined as in (4),

$$G_I(|I(\theta)\rangle) = \frac{1}{2^n} \sum_{k=0}^{2^{2n}-1} |c_k\rangle \otimes G(|k\rangle), \quad (4)$$

where $G(|k\rangle)$ for $k = 0, 1, \dots, 2^{2n} - 1$ are the unitary transformations performing geometric exchanges based on the vertical and horizontal locations. The performance of the geometric transformations on quantum images, G_I , is based on the function, G , on the computational basis vectors. The general structure of circuits for geometric transformations on FRQI images is shown in Fig.2.

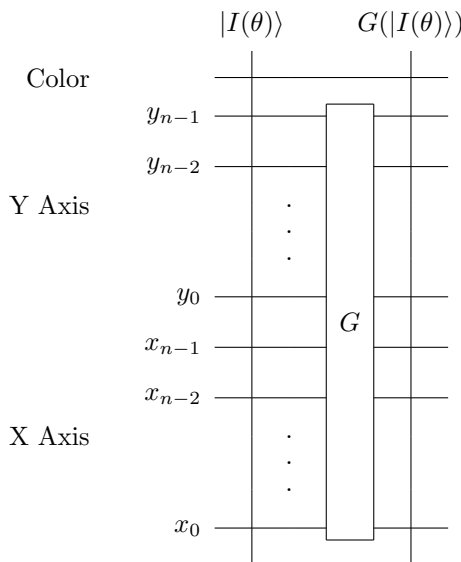


Figure 2: General circuit design for geometric transformations on quantum images

3 Two-point swapping operations

In classical image processing two-point swapping is one of the fundamental operations. However, this kind of op-

eration has not been introduced in quantum image processing because of the lack of a suitable representation for the quantum image. Based on the FRQI representation we can construct the quantum circuit for the two-point swapping operations. But let us start with the definition of the two-point swapping operation.

Definition 1. The two-point swapping operation on FRQI quantum images between two positions i, j is the operation S_I which when applied on $|I(\theta)\rangle$ in (1) produces the output of the following form

$$S_I(|I(\theta)\rangle) = \frac{1}{2^n} \sum_{k=0}^{2^{2n}-1} |c_k\rangle \otimes S(|k\rangle), \quad (5)$$

where $S(|k\rangle) = |k\rangle, k \neq i, j$ and $S(|i\rangle) = |j\rangle, S(|j\rangle) = |i\rangle$, i.e.,

$$S = |i\rangle\langle j| + |j\rangle\langle i| + \sum_{k \neq i, j} |k\rangle\langle k|. \quad (6)$$

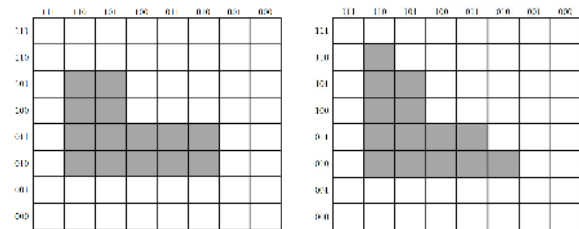


Figure 3: An example of two-point swapping operation

Figure 3 shows an example of two-point swapping operation in which the operation swaps the points $|110\rangle|110\rangle$ and $|011\rangle|010\rangle$. From the definition 1 we can reduce the operation S_I on the FRQI images $|I(\theta)\rangle$ to the operation $S(|k\rangle)$, for $k = 0, 1, \dots, 2^{2n} - 1$. For generalization, we will discuss the performance of S over the superposition of $|k\rangle$, for $k = 0, 1, \dots, 2^{2n} - 1$, that is $|K\rangle = \sum_{k=0}^{2^{2n}-1} a_k |k\rangle$.

In the quantum circuit model, a complex transform is broken down into simpler gates, i.e., single qubit, controlled two and three qubit gates, such as NOT, Hadamard, CNOT, and Toffoli gates which are shown in Fig. 4.

Note 1. The notation $C^{m-2}(\sigma_x)$ has been used for the generalized control NOT gates, where $m - 2$ indicates the number of control wires of the gates. Corollary 7.3 and Corollary 7.4 in [1] show that these gates can be constructed by Toffoli gates on a m -qubit circuit ($m \geq 5$) and the number of Toffoli gates is $8(m - 5)$ when $m \geq 7$.

The examples for Note 1 with $m = 5$ and $m = 7$ are shown in Fig. 5 and Fig. 6 respectively. These results are used in the proof of Lemma 2.

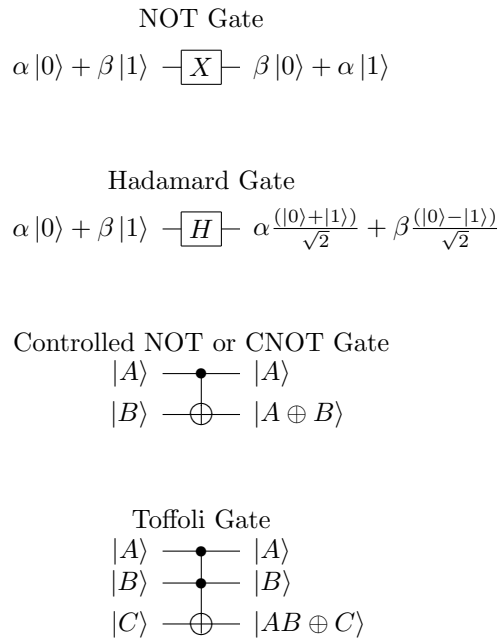


Figure 4: NOT, Hadamard, CNOT, and Toffoli gates.

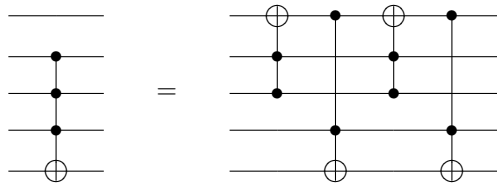


Figure 5: The $C^3(\sigma_x)$ can be constructed by 4 Toffoli gates on a 5-qubit circuit.

Lemma 1. The two-point swapping operation S for positions i, j as in (4) can be constructed by NOT, CNOT and Toffoli gates.

Figure 7 shows an example of two-point swapping circuit, that can be built from Toffoli gates.

Proof. We prove the lemma by induction.

- For $n = 0$: it is trivial since only one point in the FRQI image exists.
- For $n = 1$: the FRQI images include four points, encoded as $|00\rangle, |01\rangle, |10\rangle, |11\rangle$. There are six possible two-point swapping operations, S , between these four positions. The superposition of $|k\rangle$, for $k = 0, 1, \dots, 2^{2n} - 1$, in this case is $|K\rangle = \sum_{k=0}^{k=3} a_k |k\rangle$. These operations can be constructed by NOT and CNOT gates as in Fig. 9.
- For $n = 2$: the FRQI images contain 16 points, $|0000\rangle, |0001\rangle, \dots, |1111\rangle$. These points can be di-

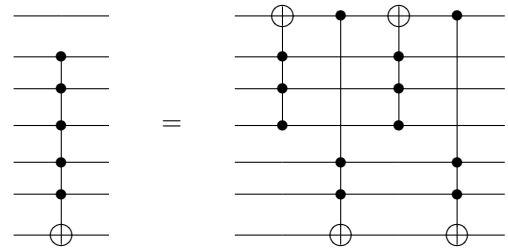


Figure 6: The $C^5(\sigma_x)$ can be constructed by 4 $C^3(\sigma_x)$ gates on a 7-qubit circuit.

Swapping between $|111011\rangle$ and $|101111\rangle$

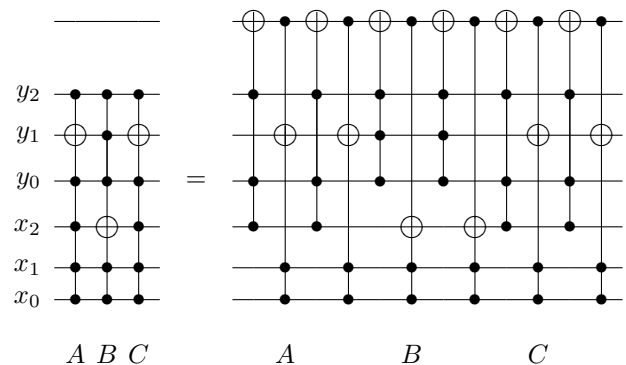


Figure 7: Example of two-point swapping operation between $|111011\rangle$ and $|101111\rangle$. Each $C^5(\sigma_x)$ in groups A, B, C can be simulated by 4 $C^3(\sigma_x)$ as in Fig. 7 and again each $C^3(\sigma_x)$ can be simulated by 4 Toffoli gates as in Fig. 6. Therefore, the swapping operation can be simulated by 16 Toffoli gates.

vided into four blocks in the form $|0y_00x_0\rangle, |0y_01x_0\rangle, |1y_00x_0\rangle$ and $|1y_01x_0\rangle$, each block includes four points. If the points at positions encoded by $|i\rangle = |y_1^i y_0^i x_1^i x_0^i\rangle, |j\rangle = |y_1^j y_0^j x_1^j x_0^j\rangle$ are in the same block, which means $y_1^i = y_1^j$ and $x_1^i = x_1^j$, we can use the circuits explained in the case $n = 1$ for the y_0 and x_0 qubits with the controlled conditions from the y_1 and x_1 qubits, which indicate the location of the block, to achieve the operation. In doing that, we use one two-point swapping on a 2-qubit system with two controlled conditions. If the points are not in the same block, we first swap the point in position $|j\rangle = |y_1^j y_0^j x_1^j x_0^j\rangle$ with a point $p = |y_1^i y_0^i x_1^i x_0^i\rangle$ in the same block with the point in position $|i\rangle = |y_1^i y_0^i x_1^i x_0^i\rangle$ by using the circuits explained in the case of $n = 1$ for the qubit y_1 and qubit x_1 under the controlled condition from the y_0 and x_0 qubits. Secondly we perform two-point swapping operation for the points i, j since they are in same block. Finally, we use two-point swapping on the qubit y_1 and qubit x_1 to exchange the points j, p . In short, we use three two-point

swapping on a 2-qubit system with two controlled conditions to complete a two-point swapping on a 4-qubit system when i, j are in different blocks. Therefore, two-point swapping, S , in the case $n = 2$ can be constructed by NOT, CNOT and Toffoli gates.

- For $n > 2$: assume that we have the two-point swapping circuits constructed by NOT, CNOT and Toffoli gates for $n - 1$ FRQI images. We denote the computational basis of the $2n$ -qubit system by $|y_{n-1}y_{n-2} \dots y_0x_{n-1}x_{n-2} \dots x_0\rangle$. The n FRQI images can be divide into 4 subimages in form

$$|0y_{n-2} \dots y_00x_{n-2} \dots x_0\rangle,$$

$$|0y_{n-2} \dots y_01x_{n-2} \dots x_0\rangle,$$

$$|1y_{n-2} \dots y_00x_{n-2} \dots x_0\rangle,$$

and

$$|1y_{n-2} \dots y_01x_{n-2} \dots x_0\rangle.$$

If the points at positions i, j encoded by $|i\rangle = |y_{n-1}^i y_{n-2}^i \dots y_0^i x_{n-1}^i x_{n-2}^i \dots x_0^i\rangle$ and $|j\rangle = |y_{n-1}^j y_{n-2}^j \dots y_0^j x_{n-1}^j x_{n-2}^j \dots x_0^j\rangle$ are in the same block, which means $y_{n-1}^i = y_{n-1}^j$ and $x_{n-1}^i = x_{n-1}^j$, we can use the circuits in the case $n - 1$ size with two controlled conditions from the y_{n-1} and x_{n-1} qubits to achieve the operation. If the points are not in the same block, we first swap the point j in the position encoded by $|j\rangle = |y_{n-1}^j y_{n-2}^j \dots y_0^j x_{n-1}^j x_{n-2}^j \dots x_0^j\rangle$ with the point p at the position encoded by $|p\rangle = |y_{n-1}^p y_{n-2}^p \dots y_0^p x_{n-1}^p x_{n-2}^p \dots x_0^p\rangle$ by using the circuits in the case of $n = 1$ size for the qubit y_{n-1} and qubit x_{n-1} with $2(n - 1)$ controlled conditions from y_k, x_k qubits ($k = 0, 1, \dots, n - 2$). Secondly we perform two-point swapping operation for the points i, j as explained in the case when they are in same block. Finally, we use two-point swapping on the qubit y_{n-1} and qubit x_{n-1} to exchange the points j, p . In short, the two-point swappings, S , in the case $n > 2$ can be constructed by NOT, CNOT and Toffoli gates.

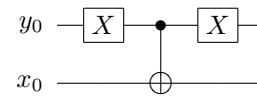
□

Remark 1. With the swapping method explained in Lemma 2, the circuit that contains the largest number of basis gates for swapping two points encoded by $|i\rangle$ and $|j\rangle$ on n -size FRQI images is the circuit for the swapping between $|0\rangle$ and $|2^{2n} - 1\rangle$.

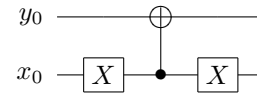
Proof. By inspection. □

Theorem 1. The complexity of two-point swapping operation on n -size FRQI images ($n \geq 2$) is $O(n^2)$.

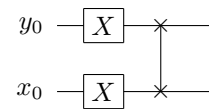
swapping $|00\rangle$ and $|01\rangle$



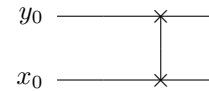
swapping $|00\rangle$ and $|10\rangle$



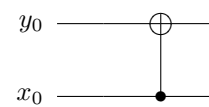
swapping $|00\rangle$ and $|11\rangle$



swapping $|01\rangle$ and $|10\rangle$



swapping $|01\rangle$ and $|11\rangle$



swapping $|10\rangle$ and $|11\rangle$

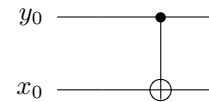


Figure 8: Swapping on 2-qubit systems.

Proof. Using the Remark 1, the complexity of two-point swapping operation on n -size FRQI images in the worst case is to swap $|0\rangle$ and $|2^{2n} - 1\rangle$. There are three groups, A, B, C in the circuit for such swapping, the example of $n = 2$ is explained in Fig. 10. The block A transforms from $|11 \dots 1\rangle|11 \dots 1\rangle$ to $|0 \dots 01\rangle|0 \dots 01\rangle$, group B swaps $|0 \dots 01\rangle|0 \dots 01\rangle$ and $|0 \dots 00\rangle|0 \dots 00\rangle$ and finally the group C transforms from $|0 \dots 01\rangle|0 \dots 01\rangle$ to $|11 \dots 1\rangle|11 \dots 1\rangle$. The group A can be divided into $n - 1$ steps to transform from $|11 \dots 1\rangle|11 \dots 1\rangle$ to $|01 \dots 1\rangle|01 \dots 1\rangle$ in first step, then from $|01 \dots 1\rangle|01 \dots 1\rangle$ to $|001 \dots 1\rangle|001 \dots 1\rangle$ in the second step, and so on. Each step in group A contains $2 C^{2n-2}(\sigma_X)$, $3 C^{2n-1}(\sigma_X)$ and NOT gates. The group C transformation is similar to group A. That of group B contains $2 C^{2n-2}(\sigma_X)$, $3 C^{2n-1}(\sigma_X)$ gates and NOT gates. Using Note 1, the

number of Toffoli gates to simulate $2(2n - 1) C^{2n-2}(\sigma_X)$ and $3(2n - 1) C^{2n-1}(\sigma_X)$ gates is $O(n^2)$. Each Toffoli gate can be simulated by 9 single qubit and 6 CNOT gates as in Fig. 5 and the number of NOT gates in the circuit is $4(n - 1)$. Hence, the total number of basis gates in the circuit is $O(n^2)$. \square

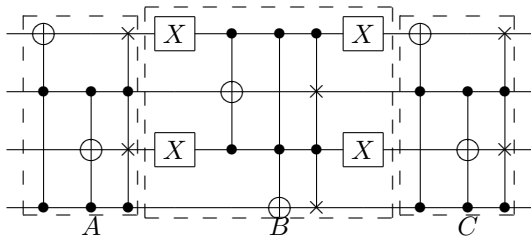


Figure 9: The two-point swapping operation can be divided into three groups A, B, C.

4 Flip and co-ordinate swap circuits

Flip and coordinate swap are fundamental operations in classical image processing. The flipping operation on FRQI quantum images is defined as follows;

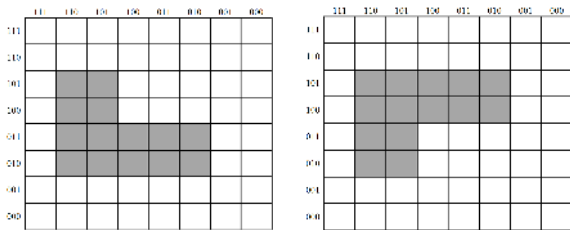


Figure 10: Image flipping along X axis.

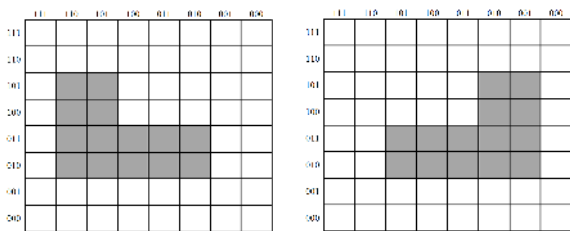


Figure 11: Image flipping along Y axis.

Definition 2. The flipping operations on FRQI quantum images along the X and Y axes are the operation F_I^X and F_I^Y which when applied on $|I(\theta)\rangle$ in (1) produces the outputs of the following form;

$$F_I^X(|I(\theta)\rangle) = \frac{1}{2^n} \sum_{k=0}^{2^{2n}-1} |c_k\rangle \otimes F^X(|k\rangle), \tag{7}$$

$$F_I^Y(|I(\theta)\rangle) = \frac{1}{2^n} \sum_{k=0}^{2^{2n}-1} |c_k\rangle \otimes F^Y(|k\rangle), \tag{8}$$

where $|k\rangle = |y\rangle|x\rangle$ and

$$F^X(|y\rangle|x\rangle) = |\bar{y}\rangle|x\rangle, \tag{9}$$

$$F^Y(|y\rangle|x\rangle) = |y\rangle|\bar{x}\rangle, \tag{10}$$

$$|x\rangle = |x_{n-1}x_{n-2} \dots x_0\rangle,$$

$$|y\rangle = |y_{n-1}y_{n-2} \dots y_0\rangle,$$

$$|\bar{x}\rangle = |\bar{x}_{n-1}\bar{x}_{n-2} \dots \bar{x}_0\rangle,$$

$$|\bar{y}\rangle = |\bar{y}_{n-1}\bar{y}_{n-2} \dots \bar{y}_0\rangle,$$

$$\bar{x}_i = 1 - x_i, \bar{y}_i = 1 - y_i,$$

$$i = 0, 1, \dots, n - 1.$$

Theorem 2. The complexity of the flipping operations F^X and F^Y as in (7) and (8) is $O(n)$ on $2n$ -qubit FRQI quantum images. quantum images.

Proof. The quantum circuits for F^X and F^Y are constructed by using n NOT gates on n qubits $y_{n-1}, y_{n-2}, \dots, y_0$ and $x_{n-1}, x_{n-2}, \dots, x_0$ respectively. In mathematical form, the circuits are expressed by the tensor product of n identity I and n Pauli X matrices. Consequently, the operations are defined as follows;

$$F^X = X^{\otimes n} \otimes I^{\otimes n}, \tag{11}$$

and

$$F^Y = I^{\otimes n} \otimes X^{\otimes n}. \tag{12}$$

\square

On FRQI quantum images the co-ordinate swapping operations are defined as follows;

Definition 3. The co-ordinate swapping operation is the operation C_I which when applied on $|I(\theta)\rangle$ in (1) produces the outputs of the following form;

$$C_I(|I(\theta)\rangle) = \frac{1}{2^n} \sum_{k=0}^{2^{2n}-1} |c_k\rangle \otimes C(|k\rangle), \tag{13}$$

where $|k\rangle = |yx\rangle$ and

$$C(|yx\rangle) = |xy\rangle. \tag{14}$$

Theorem 3. The complexity of the co-ordinate swapping operation C_I as in (13) on $2n$ -qubit FRQI quantum images is $O(n)$.

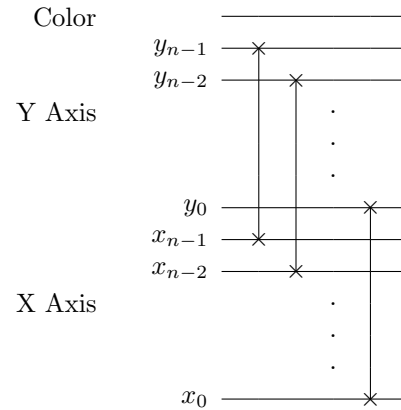
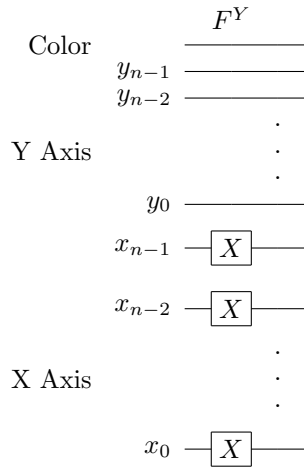


Figure 14: Co-ordinate swapping circuit.

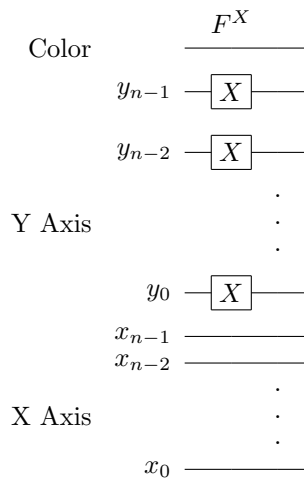


Figure 12: The circuit design of F^X and F^Y .

Proof. A swap gate, which is composed by 3 CNOT gates as shown in the Fig. 13, is used to build the circuit for C . The application of n swapping gates, G_i , on the y_i and x_i qubits for every $i = 0, 1, \dots, n - 1$ is the coordinate swapping circuit. Therefore, the operation C can be constructed by $3n$ CNOT gates. That means the complexity of the circuits is $O(n)$. \square

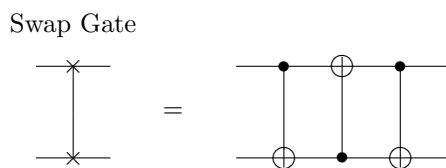


Figure 13: Swap gate can be built by three CNOT gates.

5 Orthogonal rotation circuits and other geometric transformations

Image orthogonal rotations are the image rotations with the angles 90^0 , 180^0 and 270^0 . The results from mathematics point out that the orthogonal rotations can be achieved by using flipping and coordinate swapping operations.

Definition 4. The orthogonal rotation operations on FRQI quantum images are the operations R_I^{90} , R_I^{180} , R_I^{270} which when applied on $|I(\theta)\rangle$ in (1) produces the outputs of the following form;

$$R_I^a(|I(\theta)\rangle) = \frac{1}{2^n} \sum_{k=0}^{2^{2n}-1} (\cos \theta_k |0\rangle + \sin \theta_k |1\rangle) \otimes R^a(|k\rangle), \tag{15}$$

where $a \in \{90, 180, 270\}$, $|k\rangle = |yx\rangle$ and

$$R^{90}(|yx\rangle) = |x\bar{y}\rangle, \tag{16}$$

$$R^{180}(|yx\rangle) = |\bar{y}\bar{x}\rangle, \tag{17}$$

$$R^{270}(|yx\rangle) = |\bar{x}y\rangle. \tag{18}$$

Theorem 4. The complexity of the orthogonal rotations, R^{90} , R^{180} , and R^{270} , on $2n$ -qubit FRQI quantum images is $O(n)$.

Proof. The rotations can be built from flipping and co-ordinate swapping operations as

$$R^{90} = CF^X, \tag{19}$$

$$R^{180} = F^Y F^X, \tag{20}$$

$$R^{270} = CF^Y. \tag{21}$$

\square

Other geometric transformations can be constructed from the above mentioned operations using the method that was used to achieve orthogonal rotations from flips and co-ordinate swappings. For example, we can consider

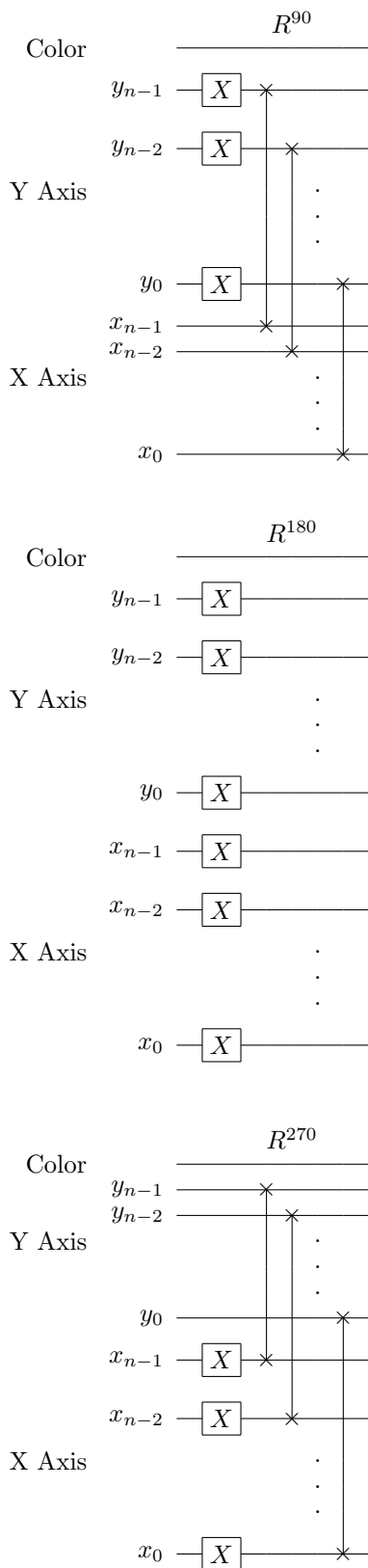


Figure 15: Rotation Circuits.

transformations that have effect on sub-areas of an image, lets say flip along X axis for right-half of the image. This kind of operations requires extra information to indicate the sub-area in which the original transformations are actually performed. From the quantum circuit model, the extra information about the sub-area is expressed in the restricting conditions used to target the sub area's by using controlled quantum gates, for example CNOT or Toffoli gate. In the example of flipping the right-half of the image along the X axis, the sub-area is the right-half and the original transformation is flip along X axis. The right-half area of an n -size image contains positions in the form $|y\rangle|1x_{n-2} \dots x_0\rangle$. We use a control condition from the qubit x_n and a flip along X axis, which includes n NOT gates as presented in section 4, in the quantum circuit design of the transformation. Therefore, the transformation can be built from n CNOT gates. Using this strategy we can create many other variants from the original proposals of flip, co-ordinate swapping and orthogonal rotations.

6 Experiments of geometric transformations on quantum images

The storage and retrieval of quantum images in FRQI representation was presented in [12]. The experiments involved simulating the quantum images on a classical computer. These simulations use linear algebra in which the complex vectors are the quantum image states and the unitary matrices are the image processing operations. The final step in these simulations is measurement which converts the quantum information into the classical information in form of probability distributions. Extracting and analyzing the distributions gives the information for retrieving the transformed images.

Using matrix operations, however, is not practical since the size of unitary matrices increases exponentially with the number of qubits. In addition, the main information for simulation is about the images only and not about the operations. In order to increase the size of images in the program memory we focus on the main information of the FRQI representation; color and positions. Therefore, for every point in the simulation of FRQI quantum images there are two arrays, named COLOR for colors $|c_k\rangle$ and POS for positions $|k\rangle$. The performance of the geometric transformations is on the POS array only and the new quantum image after the transformations is obtained by combining the POS array with its corresponding COLOR array. Table 1 shows the number of elements in each array for n -qubit (2^n -size) FRQI images. The simulation program used Matlab 2008a on a computer with Intel Core 2 Quad, 2.36 GHz CPU, 4GB Ram.

The proposed geometric transformations including flip, co-ordinate swap, orthogonal rotation, and the restricted operation to flip the right-half of the original image along

Table 1: Sizes of COLOR, POS arrays.

	COLOR	POS
Rows	2^n	2^n
Columns	1	n
Data Type	double	0,1

X axis are confirmed by simulation as shown in the Fig. 16.

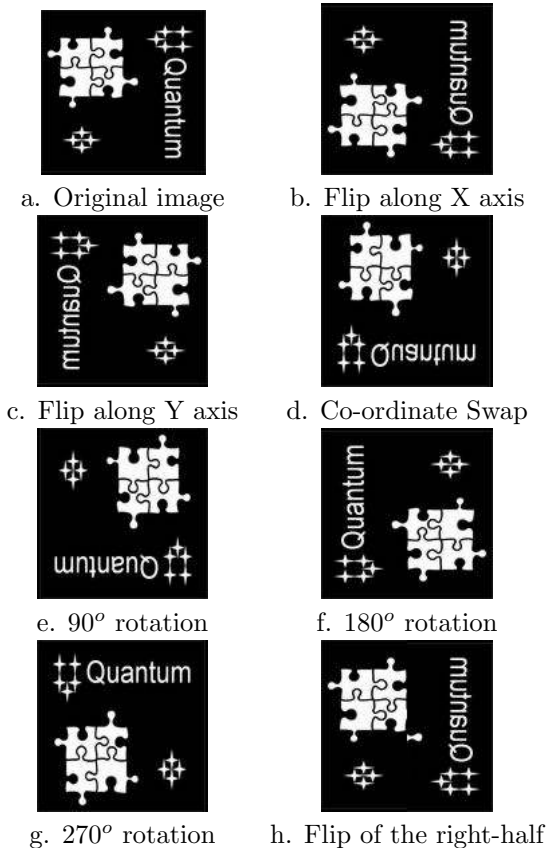


Figure 16: Confirmation of proposed geometric transformations.

For each geometric transformation on an FRQI image, the program scans and edits the content of every row in the POS array. When dealing with large images, such as 20-qubit images, scanning linearly through the POS array is not efficient. Consequently, the program uses parallel approach to speed up the whole simulation. The simulation time of NOT, CNOT, SWAP, and Toffoli gates is indicated in Table 2 and Fig. 17. The interdependence of the running time with the size of images shows the limitation of the simulation of quantum image processing. For geometric transformations, the running time increases with both the number of simple gate and the size of the images as shown in Table 3. This information is useful for designing new quantum image processing operations based on the basic gates.

Table 2: Running time (seconds) for basic gates; NOT, CNOT, SWAP, and Toffoli gates.

No. of qubits	NOT	CNOT	SWAP	Toffoli
14	0.22	0.26	0.42	0.23
16	0.33	0.37	0.85	0.27
18	0.72	0.96	2.54	0.48
20	2.20	3.34	9.50	1.40
22	8.05	12.94	38.02	5.45

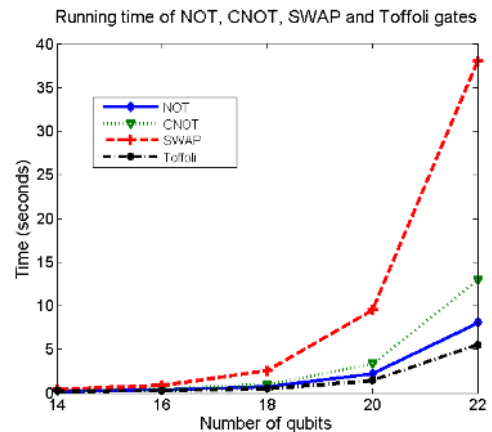


Figure 17: Simulation running time of basic gates

The next experiment is a simple image processing task. In this experiment the 512×512 input image includes four smaller 256×256 images as shown on the left side of Fig. 18. The goal is to rotate three out of the four smaller



Figure 18: The input image (left side) and the output image (right side) using in the second experiment.

images to make all the images upright and change their relative position in the input image. The output image is shown on the right side of Fig. 18.

The quantum circuit to perform such a task is shown in Fig. 19. In this circuit, there are 8 wires for X and Y axes to encode the dimensions of each of the four smaller images. The two extra wires one for each axis are used to encode the smaller 256×256 images relative to the larger 512×512 image. The circuit comprises of two blocks of

Table 3: Running time (seconds) of geometric transformations

No. of qubits	Flip	Swap	Rotation	Others
14	1.10	1.95	2.46	6.32
16	1.51	5.56	6.80	15.40
18	5.11	21.47	25.56	56.60
20	20.57	93.61	116.30	243.51
22	90.11	428.52	517.09	1116.9

geometric transformations R^{90} and restricted version of R^{270} . The R^{90} block rotates the whole image 90° clockwise. Finally, the upper-left 256×256 smaller image obtained from the previous step is rotated 270° clockwise. This is achieved by imposing additional restrictions to target and restrict the operation to that area only as seen in Fig. 19. To realize the desired output image, a middle stage is obtained after rotating the entire 512×512 image using the R^{90} operation. The output image of this stage is shown in Fig. 20. The block has two control wires on R^{270} from the extra wires which provide the information to restrict the performance of R^{270} on the upper-left corner.

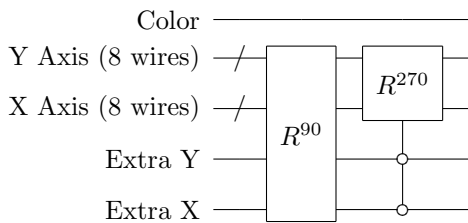


Figure 19: Quantum circuit for the application comprising two blocks of geometric transformations R^{90} and restricted version of R^{270} .



Figure 20: The image obtained from the input image after the first step.

As proven in 5, the total number of basic gates in the quantum circuit is linear with the number of qubits used to express the input image i.e. 18 qubits. To achieve the same operation, an operation has to examine each pixel in the input image and move it to a new position in the

output image, that means the complexity is equal to the size of the input image, in this case $2^9 \times 2^9$. This result shows the efficiency of geometric transformations on FRQI quantum images over similar operations on classical computers.

7 Conclusions

Geometric transformations on quantum images including two-point swapping, flip, co-ordinate swapping, and orthogonal rotations with low complexity are proposed using basic gates like NOT, CNOT, and Toffoli gates. This low complexity agrees with results for similar transformations which are also fast on classical images. The proposed operations can be divided into local and global operations according to their effect on the quantum images. From this point of view, the local operations are found to be slower than the global operations resulting from the parallelism of quantum computation. This is in contrast to classical image processing transformations. Although arbitrary geometric transformations can be constructed by two-point swapping operations, the complexity of this method is high since we are using local operations, especially for those geometric transformations that have global effect. Meanwhile, the global operations like flip, co-ordinate swapping, and orthogonal rotations are faster, that means we should think about these operations before using local operations in the design process of quantum circuits. The simulation experiments confirm all the proposed transformations. Based on the results presented in 3-5, we can restrict the basic operations on our simulation system to NOT, CNOT, and Toffoli gates. The memory space and processing speed, posed some unavoidable problems in the simulation of quantum images and their processing operations on classical computers. In order to improve the performance of the simulation system, our strategy was to reduce memory space by focusing on the effect of transformations on quantum images instead of the transformations themselves. During the analysis of the simulation system in 6, we found out that the parallelism of transformations on quantum images can be translated directly to the parallel computing methods.

As for future work, the results in this paper will be extended towards the following directions. As discussed in 3, the two-point swapping operators can be used to construct arbitrary geometric transformations. Since their complexity is $O(\log^2 N)$, we should use them as less as possible and use more operations like flip, co-ordinate swapping and rotations whose complexity is $O(\log N)$. Secondly, the problem of designing the quantum circuits with low complexity for arbitrary geometric transformations is still open and needs to be investigated using the group theory point of view. Thirdly, using geometric transformations in other applications of quantum image processing appears very promising, for example applica-

tions in quantum image watermarking, quantum image cryptography can be done by hiding secret information in the design of quantum circuits. Combining with the color related operations [18], the geometric operations can be used as major components to build full quantum image processing applications.

References

- [1] Barenco, A., Bennett, C. H., Cleve, R., DiVincenzo, D. P., Margolus, N., Shor, P., Sleator, T., Smolin, J. A., Weinfurter, H., "Elementary gates for quantum computation," *Phys. Rev. A* 52, 3457, 1995.
- [2] Beach, G., Lomont, C., Cohen, C., "Quantum image processing (quip)," *Proc. of Applied Imagery Pattern Recognition Workshop*, pp.39-44, 2003.
- [3] Caraiman, S., Manta, V. I., "New applications of quantum algorithms to computer graphics: the quantum random sample consensus algorithm," *Proc. of the 6th ACM conference on Computing frontier*, pp. 81-88, 2009.
- [4] Curtis, D., Meyer, D. A., "Towards quantum template matching," *Proc. of the SPIE*, Vol. 5161. pp. 134-141, 2004.
- [5] Feynman, R. P., "Simulating physics with computers," *International Journal of Theoretical Physics*, 21(6/7). pp. 467-488, 1982.
- [6] Fijany, A., Williams, C. P., "Quantum wavelet transform: fast algorithm and complete circuits," [arXiv:quantph/9809004](https://arxiv.org/abs/quantph/9809004), 1998.
- [7] Grover, L., "A fast quantum mechanical algorithm for database search," *Proc. of the 28th Ann. ACM Symp. on the Theory of Computing (STOC 1996)*, pp. 212-219, 1996.
- [8] Klappenecker, A., Rotteler, M., "Discrete cosine transforms on quantum computers," *Proc. of the 2nd Inter. Symp. on Image and Signal Processing and Analysis*, pp. 464-468, 2001.
- [9] Latorre, J. I., "Image compression and entanglement." [arXiv:quant-ph/0510031](https://arxiv.org/abs/quant-ph/0510031), 2005.
- [10] Lomont, C., "Quantum convolution and quantum correlation algorithms are physically impossible," [arXiv:quantph/0309070](https://arxiv.org/abs/quantph/0309070), 2003.
- [11] Lomont, C., "Quantum circuit identities," [arXiv:quantph/0307111](https://arxiv.org/abs/quantph/0307111), 2003.
- [12] Le, P. Q, Dong, F., Hirota, K., "Flexible representation of quantum images and its computational complexity analysis," *Proc. 10th Intl. Symp. on Advanced Intelligent Systems*, pp. 146-149, 2009.
- [13] Maslov, D., Dueck, G. W., Miller, D. M., Camille, N., "Quantum circuit simplification and level compaction," *IEEE Trans. on Computer-Aided Design of Integrated Circuits and Systems*, 27(3). pp. 436-444, 2008.
- [14] Monz, T., Kim, K., Hansel, W. , Riebe, M., Villar, A. S. ,Schindler, P. , Chwalla, M. , Hennrich, M., Blatt, R., "Realization of the quantum Toffoli gate with trapped ions," *Phys. Rev. Let.* 102, 040501, 2009.
- [15] Nielsen, M., Chuang, I., *Quantum computation and quantum information*, Cambridge University Press, New York, 2000.
- [16] Shor, P. W., "Algorithms for quantum computation: discrete logarithms and factoring," *Proc. 35th Ann. Symp. Foundations of Computer Science*, IEEE Computer Soc. Press, Los Almitos, CA. pp. 124-134, 1994.
- [17] Tseng, C. C., Hwang, T. M., "Quantum circuit design of 8×8 discrete cosine transforms using its fast computation on graph," *ISCAS 2005*, vol. I, pp. 828-831, 2005.
- [18] Venegas-Andraca, S. E., Ball, J. L., "Storing Images in entangled quantum systems," [arXiv:quant-ph/0402085](https://arxiv.org/abs/quant-ph/0402085), 2003.
- [19] Venegas-Andraca, S. E., Bose, S., "Storing, processing and retrieving an image using quantum mechanics," *Proc. of the SPIE Conf. Quantum Information and Computation*, pp.137-147, 2003.